

# Transcriptomic analysis of the thyroid and ovarian stroma reveals key pathways and potential candidate genes associated with egg production in ducks

Zhiyu He,<sup>#</sup> Qingliang Chen,<sup>#</sup> Qingyuan Ouyang,<sup>#</sup> Jiwei Hu, Zhengyang Shen, Bo Hu, Shenqiang Hu, Hua He, Liang Li, Hehe Liu, and Jiwen Wang<sup>1</sup>

*Farm Animal Genetic Resources Exploration and Innovation Key Laboratory of Sichuan Province, Sichuan Agricultural University, Chengdu, Sichuan 611130, China*

**ABSTRACT** The importance of thyroid-related genes has been repeatedly mentioned in the transcriptome studies of poultry with different laying performance, yet there are few systematic studies to unravel the regulatory mechanisms of the thyroid-ovary axis in the poultry egg production process. In this study, we compared the transcriptome profiles in the thyroid and ovarian stroma between high egg production (GP) and low egg production (DP) ducks, and then revealed the pathways and candidate genes involved in the process. We identified 1,114 and 733 differentially expressed genes (DEGs) in the thyroid and ovarian stroma, separately. The Gene Ontology (GO) analysis showed that a total of 504 and 189 GO terms were identified in the thyroid and ovarian stroma ( $P < 0.05$ ). Three common GO terms were identified from the top 5 GO terms with the highest significant level in two tissues, including extracellular space, calcium ion binding, and integral component of plasma membrane. The enrichment analysis of the Kyoto Encyclopedia of Genes and Genomes (KEGG) showed that 15 and 14 KEGG pathways were significantly ( $P < 0.05$ ) enriched in the thyroid and ovarian stroma, respectively. And, there

were 8 common pathways, including neuroactive ligand-receptor interaction, calcium signaling pathway, ECM-receptor interaction, PPAR signaling pathway, melanogenesis, wnt signaling pathway, vascular smooth muscle contraction, and cytokine-cytokine receptor interaction. Notably, the neuroactive ligand-receptor interaction pathway was the most significantly enriched by the DEGs both in the thyroid and ovarian stroma. The interaction among DEGs enriched in the neuroactive ligand-receptor interaction and ECM-receptor interaction suggested that the thyroid may regulate ovarian development by these genes. Through integrated analysis of the protein-protein interaction (PPI) network and KEGG pathway maps, 9 key DEGs (*PTH*, *THBS2*, *THBS4*, *CD36*, *ADIPOQ*, *ACSL6*, *PRKAA2*, *CRH*, and *PCK1*) were identified, which could play crucial roles in the thyroid to regulate ovarian function and then affect egg-laying performance between GP and DP. This study serves as a basis to explore the molecular mechanism of the thyroid affecting ovarian function and egg production in female ducks and may help to identify molecular markers that can be used for duck genetic selection.

**Key words:** duck, transcriptome, thyroid, ovarian stroma, egg production

2023 Poultry Science 102:102292

<https://doi.org/10.1016/j.psj.2022.102292>

## INTRODUCTION

The thyroid has a considerable influence on reproductive activity in female poultry (Miller et al., 1962). The traditional techniques, such as thyroid resection (Haddad and Mashaly, 1989) and hormone control (Bilezikian et al., 1980), have revealed functions of the

thyroid in early gonadal development and later egg production. Suppression of the thyroid will result in reduced egg production or even complete cessation (Lien and Siopes, 1989). In the studies on the molecular mechanisms of egg production with the support of emerging omics technology, some results laterally showed the close relationship between egg production and the thyroid. For instance, through transcriptome sequencing (RNA-seq) of the hypothalamus from chickens with different egg production, the enriched thyroid hormone signaling pathway and thyroid hormone synthesis may play important roles in regulating egg production (Ma et al., 2021). And by sequencing the hypothalamus and pituitary of turkeys with high and low egg production, the result showed that

© 2022 The Authors. Published by Elsevier Inc. on behalf of Poultry Science Association Inc. This is an open access article under the CC BY-NC-ND license (<http://creativecommons.org/licenses/by-nc-nd/4.0/>).

Received July 5, 2022.

Accepted October 19, 2022.

<sup>#</sup>These authors have contributed equally to this work.

<sup>1</sup>Corresponding author: [wjw2886166@163.com](mailto:wjw2886166@163.com)

the differentially expressed genes (DEGs) were enriched in the hypothalamus-pituitary-thyroid axis (Brady et al., 2020). In addition, transcriptome analysis of the granulosa layer of the largest follicle and the fifth-largest follicle (F5), theca internal layer of the F5 follicle, and small white follicle samples from turkeys with different egg production implied thyroid hormone transporters and thyroid hormone receptors may be involved in regulating the difference (Brady et al., 2021). In ducks, the DEGs involved in regulating different egg production are also enriched in the thyroid hormone signaling pathway (Bao et al., 2020). Although some studies have shown that the thyroid is very important for normal reproductive activities of poultry, until now, the molecular mechanism of thyroid affecting ovarian function and egg production level has yet to be fully elucidated.

The ovary is an important target organ of the thyroid-related hormone (Sechman, 2013), and also the site of follicle growth and development. It is estimated that there are about 480,000 oocytes in chicken's ovary, but only a few hundred oocytes will be selected to mature and ovulate (Onagbesan et al., 2009), and the function of the ovary will directly affect egg production. In the research on egg-laying performance, people often collected ovary or its components to explore the molecular mechanisms. The ovaries of Ninghai indigenous chickens were collected in the early, peak, and late stages of egg-laying for sequencing, nine genes (*LRP8*, *BMP6*, *ZP4*, *COL4A1*, *VCAN*, *INHBA*, *LOX*, *PTX3*, and *IHH*) were identified as candidate genes for regulating egg production, and four pathways related to egg-laying performance were determined (Huang et al., 2022). The ovarian stroma of each individual was collected and sequenced, which revealed the key role of the 5-hydroxytryptamine receptor in regulating the egg production of geese (Ouyang et al., 2020). In ducks, the ovaries of black Muscovy ducks and white Muscovy ducks were selected for transcriptome study, then 9 related candidate genes were identified (Bao et al., 2020). Although many studies have selected ovaries for sequencing to explore the molecular mechanisms regulating egg-laying performance, most of them compared ovaries with hypothalamic or pituitary transcripts (Bello et al., 2021; Yan et al., 2022) or ovarian transcripts at different egg-laying stages (Zhu et al., 2017; Hu et al., 2021), few studies selected the thyroid and ovary or ovarian components for combined transcriptome analysis. To further unravel the molecular mechanisms regulating egg-laying performance, it is necessary to perform transcriptomic analysis of the thyroid and ovary.

The importance of thyroid-related genes has been repeatedly mentioned in transcriptomic studies of poultry ovaries with high and low egg production, yet there is a lack of combined transcriptome study to unravel the regulatory mechanisms of the thyroid-ovary axis on the poultry egg production process. In this experiment, there is a significant difference between high egg production (GP) and low egg production (DP) ducks, which may be related to the regulation of the thyroid on the ovary. Therefore, we performed RNA-seq of the thyroid and

ovarian stroma from GP and DP. The purpose is to identify the candidate genes and molecular mechanisms leading to different egg-laying performances of ducks. These results will provide new and comprehensive insights into the potential molecular mechanisms by which the thyroid regulates the ovary, and thus affects egg-laying performance.

## MATERIALS AND METHODS

### Experimental Animals

All experimental procedures that involved animal manipulation were approved by the Faculty Animal Care and Use Committee of Sichuan Agricultural University (Ya'an, Sichuan, China) under permit no. DKY20170913.

A total of 156 female ducks (Tianfu Nonghua speckled duck) came from the Waterfowl Breeding Experimental Farm of Sichuan Agricultural University (Ya'an, Sichuan, China). The experimental ducks were raised on the ground and transferred to a single cage at the age of 120 days. The number of individual eggs from 130 d to 254 d was recorded daily. In this study, the top 20% of individuals with the highest number of eggs were defined as GP and the last 20% of individuals with the lowest number of eggs were defined as DP. One-way ANOVA showed that there was a significant difference in egg production between GP and DP ( $P < 0.01$ ).

### Sample Collection

Three healthy ducks with similar egg-laying mode, body weight, age of the first egg, and physiological condition were selected from each group as the final experimental animals. The selected experimental ducks were killed by inhaling carbon dioxide and cervical dislocation after fasting for about 12 h. Quickly collecting the left thyroid and intact ovary, then removing the visible follicles on the ovarian surface. The thyroid and ovarian stroma were collected and snap-frozen into liquid nitrogen. All samples were stored at  $-80^{\circ}\text{C}$  for subsequent experiments.

### RNA Extraction and Sequencing

The thyroid and ovarian stroma were ground under liquid nitrogen and the powdered tissue was transferred to a RNase-free tube prechilled with 1 mL Trizol (Invitrogen, Massachusetts, CA). After lysis at room temperature for 5 min, centrifuge the sample at  $4^{\circ}\text{C}$  for 5 min at  $13,000 \times g$ . Aspirate the supernatant, add 200  $\mu\text{L}$  of chloroform, react at room temperature for 5 min, and centrifuge at  $4^{\circ}\text{C}$  for 5 min at  $13,000 \times g$ . Get the upper aqueous phase, add 400  $\mu\text{L}$  of anhydrous ethanol and 10  $\mu\text{L}$  of magnetic beads, mix well, and leave for 5 min. Use the magnetic stand to adsorb the magnetic beads, aspirate the supernatant, add 700  $\mu\text{L}$  of 75% ethanol and mix thoroughly, and repeat twice. The magnetic beads

were dried at room temperature for 10 min, and then eluting the RNA. The genomic DNA was removed by DNase I (Takara, Dalian, China), and the RNA integrity was identified by Agilent Bioanalyzer 2100 (Agilent Technologies, Santa Clara, CA). Major-bio (Shanghai, China) constructed an Illumina PE library using RNA with an average RIN value of 9.85 (9.7–10), and completed  $2 \times 150$ bp RNA-seq with NovaSeq 6000 sequencing platform. The RNA-seq data of this study could be obtained on NCBI (National Center for Biotechnology Information) (BioProject ID PRJNA791517). The clean reads were obtained after the filtration of low-quality reads using standard quality control by FastaQC software.

### Transcriptome Alignment and Assembly

The clean reads were mapped to the duck reference genome (GCA\_015476345.1) using HISAT2 software (version 2.2.1) (Kim et al., 2015). The output SAM (sequence alignment/mapping) files were converted to BAM (binary alignment/mapping) files and sorted by the SAM tools (version 1.10) (Li et al., 2009). Then, the expressions of each transcript were calculated by featureCounts (version 1.6.0) (Liao et al., 2014) and converted to transcripts per million (TPM) for normalization.

### Identification and Functional Analysis of DEGs

The DEGs between groups were identified by DESeq2 and the screening criteria were  $|\log_2\text{foldchange}| > 1$ ,  $P < 0.05$ . The online website KOBAS 3.0 was used to analyze the Gene Ontology (GO) functions and Kyoto Encyclopedia of Genes and Genomes (KEGG) functions (<http://kobas.cbi.pku.edu.cn/kobas3/?t=1>). Using STRING 11.5 database (<http://string-db.org/>) to identify the relationship between DEGs, and using Cytoscape software (version 3.7.1) for network visualization.

### Quantitative Real-Time PCR Validation

Nine DEGs were selected for quantitative real-time PCR (qRT-PCR) to verify the RNA-seq results. The total RNA extracted from the thyroid and ovarian stroma was reverse transcribed into cDNA by HiScriptIII RT SuperMix for qPCR (+gDNA wiper) (Vazyme, Nanjing, China). The reverse transcription was performed in a total volume of 20  $\mu$ L, which contained: 4  $\times$  gDNA wiper Mix 4  $\mu$ L, RNA 2  $\mu$ L, ddH<sub>2</sub>O 10  $\mu$ L, 5  $\times$  No RT Control Mix 4  $\mu$ L and the conditions are as follows: 42°C for 2 min; 37°C for 15 min and 85°C for 5 s. Primer 5.0 was used to design primers (Table 1), and BLAST was used to determine the specificity of primers. The qRT-PCR was performed using Bio-Rad CFX96 real-time PCR detection system (Bio-Rad, Hercules, CA, USA), and each sample was repeated three times and choosing  $\beta$ -Actin and GAPDH as internal reference genes for normalization. The qRT-PCR was performed in a total volume of 20  $\mu$ L, which contained: Taq Pro

**Table 1.** Primer sequences used in this study.

Gene Name	Sequence (5'-3')	Product length (bp)
<i>PTH-F</i>	CTCTGATGGAAGACCAATGATGAAA	84
<i>PTH-R</i>	TCCACAGTGTGTCGATGCTC	
<i>THBS2-F</i>	GGCTGTTGTGGCTTGCTGTCTT	164
<i>THBS2-R</i>	TGCTGGGATAGTGGGATCTGGAC	
<i>CD36-F</i>	TGGGAAGGTTACTGTGATTTGGTT	141
<i>CD36-R</i>	CACATTCTGTTTGGCCCTGGAAG	
<i>CRHF</i>	CAACCTCAACAAGAGACCCG	252
<i>CRHR</i>	TCTCGGAGGAGGTGGAAAAGTC	
<i>ADIPOQ-F</i>	CAAGGTCAGCCTCTACAAGAAGGA	197
<i>ADIPOQ-R</i>	AGCCCATGAAAAGTGGAAATCGT	
<i>ACSL6-F</i>	GGCTGTGTCCGCATGATAGT	173
<i>ACSL6-R</i>	GGGGCTCCTACATGACCTGA	
<i>PCK1-F</i>	TCCCAACTCACGGTTCTGC	176
<i>PCK1-R</i>	TGGCTGCTCCTATAAATACTCCAT	
<i>PRKAA2-F</i>	TGCCACCTTTGATAGCGG	141
<i>PRKAA2-R</i>	CCATAATGTCATAGGGCTTGCT	
<i>MAPK12-F</i>	TGGTCACAAGGTGGTACAGAGC	144
<i>MAPK12-R</i>	GGTCCAGATGATCGTTTCCCT	
$\beta$ - <i>ACTIN-F</i>	GCTATGTCGCCCTGGATTTC	168
$\beta$ - <i>ACTIN-R</i>	CACAGGACTCCATACCCAAGAA	
<i>GAPDH-F</i>	GTCTCTGTGCTGGACCTGAC	113
<i>GAPDH-R</i>	GTGTATGCCAGGATGCCCTT	

Universal SYBR qPCR Master Mix (Vazyme, Nanjing, China) 10  $\mu$ L, 0.4  $\mu$ L of each primer, cDNA 2  $\mu$ L, ddH<sub>2</sub>O 7.2  $\mu$ L. The qPCR amplification conditions are as follows: 95°C for 30 s; 40 cycles of 95°C for 10 s and 60°C for 30 s. The  $2^{-\Delta\Delta CT}$  method was used for the normalization of the qRT-PCR results, after which the normalized data was used for statistical analysis.

### Statistical Analysis

One-way ANOVA was performed to compare the differences in egg-laying data between GP and DP, and Spearman's correlation coefficient was calculated to analyze the correlations between qRT-PCR and RNA-seq results. The results with  $P < 0.05$  were statistically significant. All statistical analyses were carried out using the SPSS 27.0 software.

## RESULTS AND ANALYSIS

### Overview of RNA-seq and Identification of the DEGs

A total of 310,180,660 raw reads were obtained from the 12 samples, and an average of 25,637,289 clean reads were obtained from each sample after the strict screening. The Q20, Q30, and mapping rates were within 98.12% to 98.62%, 94.45% to 95.80%, and 89.56% to 91.35%, respectively, and the sequencing quality was acceptable for subsequent analysis (Table 2).

We identified 1,114 DEGs in the thyroid, including 809 up-regulated DEGs and 305 down-regulated DEGs (Figure 1a). Meanwhile, in the ovarian stroma, a total of 733 DEGs were identified, including 377 up-regulated DEGs and 356 down-regulated DEGs (Figure 1b). There

**Table 2.** Basic information of mRNA sequencing data of all samples in this study.

Sample	Raw Reads	Clean Reads	Q20 (%)	Q30 (%)	GC Content (%)	Mapping rate (%)
G-T1	24142976	23952856	98.51	95.45	47.60	90.78
G-T2	24911939	24718168	98.57	95.66	48.96	90.03
G-T3	22406241	22158214	98.12	94.45	48.20	90.91
D-T1	26395135	26184583	98.51	95.46	48.40	90.63
D-T2	23626239	23453064	98.57	95.61	47.90	90.44
D-T3	21315378	21149316	98.58	95.60	48.75	90.68
G-O1	25846618	25640611	98.56	95.66	50.01	90.71
G-O2	24706057	24519859	98.55	95.58	48.83	91.29
G-O3	35418703	35078182	98.59	95.80	50.96	90.07
D-O1	26013726	25809151	98.57	95.68	50.01	89.56
D-O2	28031172	27834834	98.62	95.54	49.16	91.35
D-O3	27366476	27148641	98.58	95.67	51.24	90.41

Abbreviations: D-O, low egg production-ovarian stroma; D-T, low egg production-thyroid; G-O, high egg production-ovarian stroma; G-T, high egg production-thyroid.

were 112 DEGs commonly identified in the thyroid and ovarian stroma (Figure 1c). The TPM hierarchical clustering map demonstrated the thyroid (Figure 1d) and ovarian stromal (Figure 1e) gene expression patterns between GP and DP and showed the reliability of the gene sets.

### Functional Enrichment Analysis of the Identified DEGs

To further demonstrate the function of the DEGs in the thyroid and ovarian stroma between GP and DP, we performed GO and KEGG enrichment analyses. A total of 504 GO terms were identified in the thyroid, including 346 biological processes (BP), 62 cellular components (CC), and 96 molecular functions (MF) ( $P < 0.05$ ) (Figure 2a). Meanwhile, 189 GO terms were identified in the ovarian stroma, including 123 BP, 32 CC, and 34 MF (Figure 2c). Furthermore, through analyzing the top 5 terms with the highest significant level in 2 tissues, we identified 3 common terms, including extracellular space, calcium ion binding, and integral component of plasma membrane.

Based on KEGG pathway enrichment analysis, 105 pathways were identified in the thyroid, of which 15 pathways were significantly enriched ( $P < 0.05$ ), including neuroactive ligand-receptor interaction, calcium signaling pathway, cell adhesion molecules (CAMs), steroid biosynthesis, ECM-receptor interaction, PPAR signaling pathway, glycosaminoglycan biosynthesis-chondroitin sulfate/dermatan sulfate, melanogenesis, MAPK signaling pathway, wnt signaling pathway, vascular smooth muscle contraction, mucin type O-glycan biosynthesis, N-Glycan biosynthesis, cytokine-cytokine receptor interaction, and metabolic pathways (Figure 2b). And 71 pathways were identified in the ovarian stroma, of which 14 pathways were significantly enriched ( $P < 0.05$ ), including neuroactive ligand-receptor interaction, ECM-receptor interaction, focal adhesion, adipocytokine signaling pathway, cytokine-cytokine receptor interaction, calcium signaling pathway, melanogenesis, wnt signaling pathway, PPAR

signaling pathway, vascular smooth muscle contraction, apelin signaling pathway, FoxO signaling pathway, regulation of actin cytoskeleton, and tyrosine metabolism (Figure 2d).

Subsequently, 8 common pathways enriched by DEGs were identified in the thyroid and ovarian stroma, including neuroactive ligand-receptor interaction, calcium signaling pathway, ECM-receptor interaction, PPAR signaling pathway, melanogenesis, wnt signaling pathway, vascular smooth muscle contraction, and cytokine-cytokine receptor interaction. It is worth noting that the neuroactive ligand-receptor interaction pathway was the most significantly enriched by the DEGs in 2 tissues.

### Possible Molecular Mechanisms of Thyroid Regulation in Ovarian Development

According to the results of GO and KEGG enrichment analysis, it is speculated that the neuroactive ligand-receptor interaction is an important way for the thyroid to regulate ovarian function. The PPI of genes enriched in this pathway of 2 tissues were mapped by using String and Cytoscape software (Figure 3a), the *PTH* was found to be differentially expressed at the highest fold change up to 12.9, and it was differentially expressed in the thyroid. The node number of *CRH* was the highest, and it was differentially expressed in the ovarian stroma. In addition, genes involved in the ECM-receptor interaction from the thyroid that encode extracellular matrix components were up-regulated (*LAMA3*, *CHAD*, *THBS2*, *THBS4*), and this pathway may activate the PPAR signaling pathway in the ovarian stroma through *THBS2*, *THBS4*, and *CD36*. The *CD36* is located upstream of the PPAR signaling pathway to regulate the downstream genes involved in lipid metabolism and adipocyte differentiation, among which, *ACSL6* and *ADIPOQ* are up-regulated in the ovarian stroma while *PCK1* is down-regulated. The *ACSL6*, *ADIPOQ*, and *PCK1* are involved in fatty acid transport, adipocyte differentiation, and gluconeogenesis, separately. The possible regulatory relationships are shown in Figure 3b.



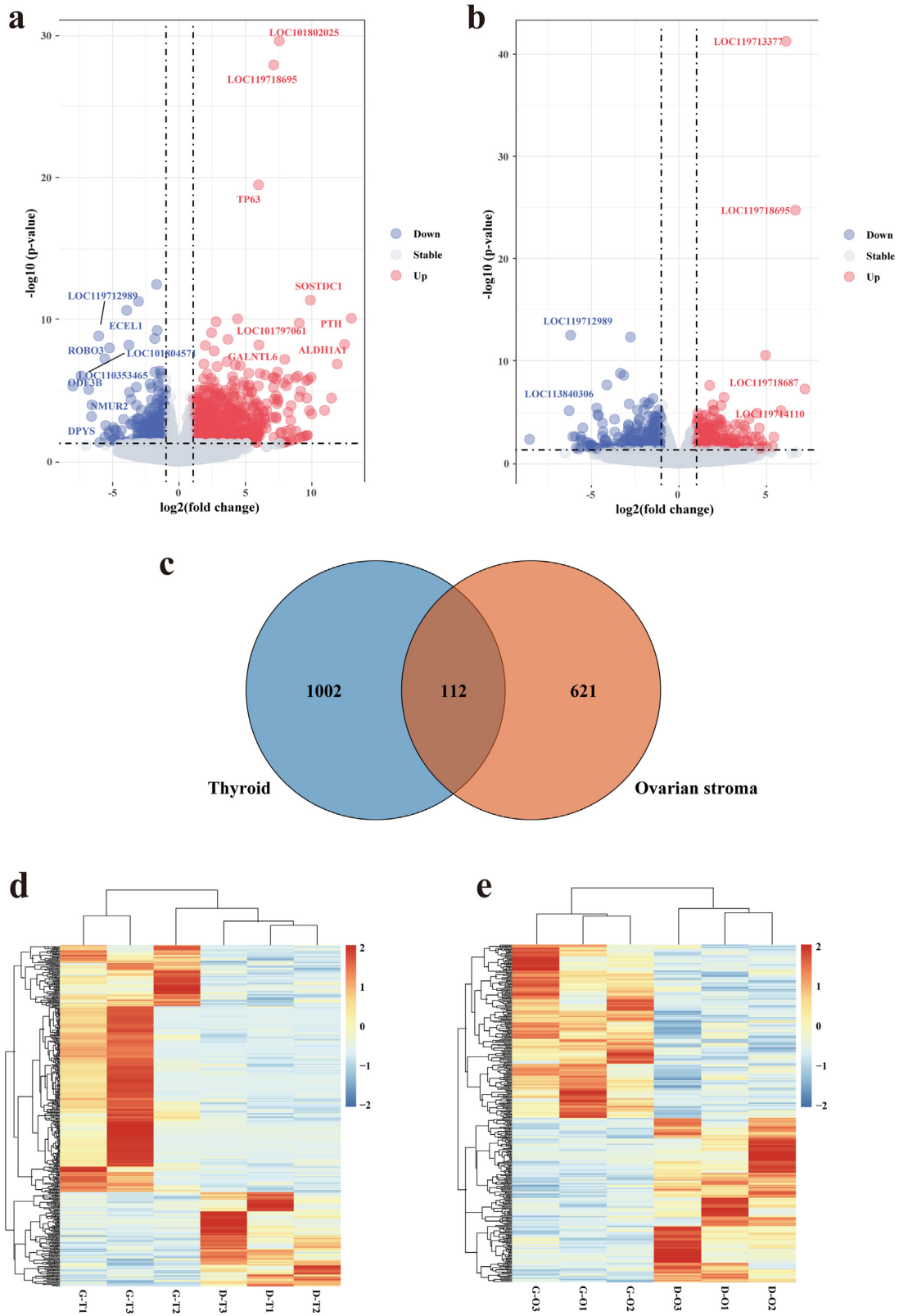


**Figure 1.** Transcriptome variation characteristics of each tissue between GP and DP groups. Volcano map exhibited DEGs of the thyroid (a) and ovarian stroma (b). Venn plot revealed 112 intersect genes between GP and DP (c). Hierarchical clustering of DEGs in the thyroid (d) and ovarian stroma (e). Abbreviations: DEG, differentially expressed gene; D-O, low egg production-ovarian stroma; DP, low egg production; GP, high egg production; G-T, high egg production-thyroid; D-T, low egg production-thyroid; G-O, high egg production-ovarian stroma.

### Validation of RNA-seq Results by qRT-PCR

To verify the RNA-seq results, nine DEGs were selected to perform qRT-PCR. There were three genes

up-regulated in the thyroid (*PTH*, *THBS2*, *CD36*), three genes up-regulated in the ovarian stroma (*ADIPOQ*, *ACSL6*, *PRKAA2*), and three genes down-regulated in the ovarian stroma (*CRH*, *PCK1*, *MAPK12*).

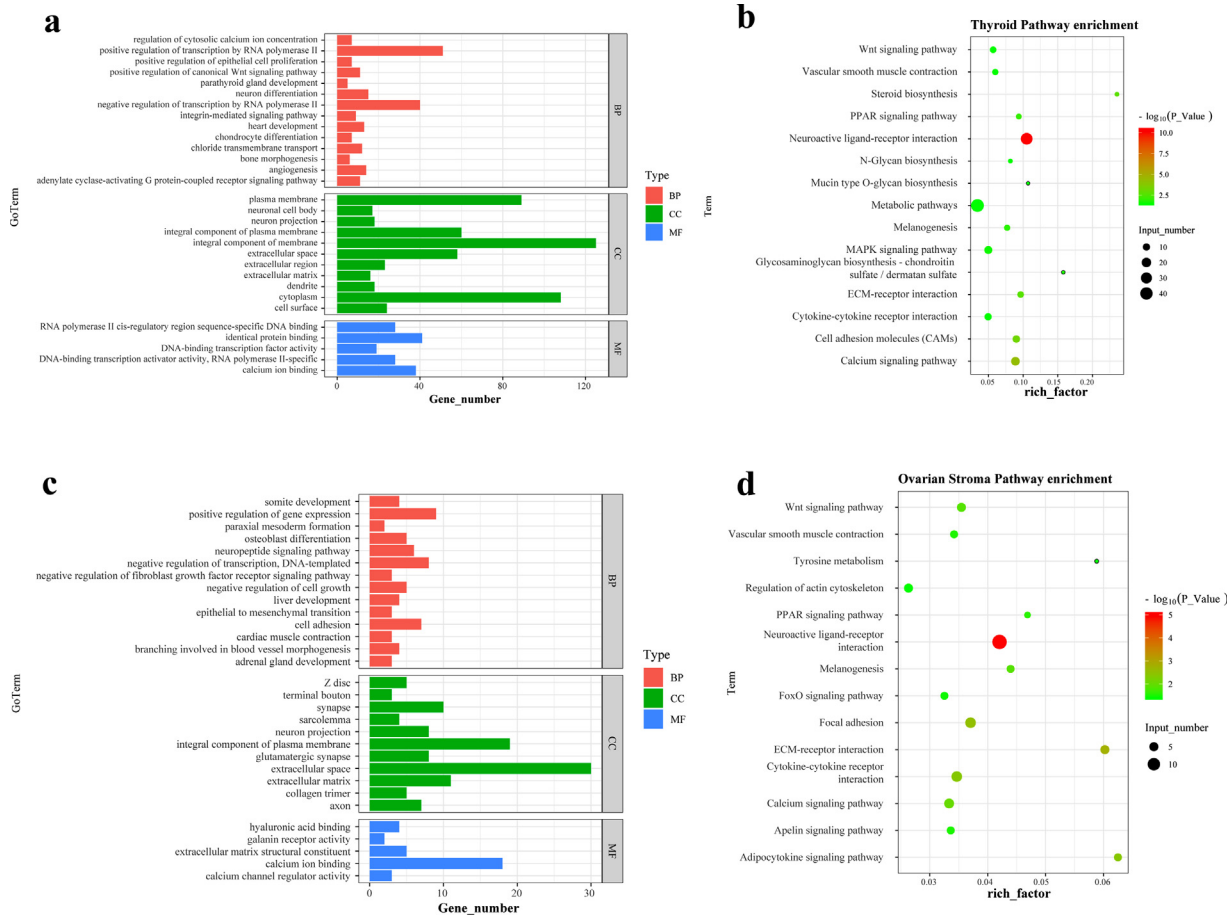


**Figure 2.** GO terms and KEGG pathways enriched by DEGs. Histogram of top 30 GO terms enrichment of DEGs in the thyroid (a) and ovarian stroma (c). The bubble plots showed that the KEGG pathways significantly enriched ( $P < 0.05$ ) in the thyroid (b) and ovarian stroma (d). Abbreviations: GO, Gene Ontology; KEGG, Kyoto Encyclopedia of Genes and Genomes; DEG, differentially expressed gene; BP, biological processes; CC, cellular components; MF, molecular functions.

Normalized with  $\beta$ -actin and *GAPDH*, the expression profiles of nine key genes generated from qRT-PCR corresponded to the RNA-seq results (Figure 4a), the linear regression and Spearman correlation coefficient ( $r_s = 0.967$ ) (Figure 4b) indicated the consistency between qRT-PCR and RNA-seq.

## DISCUSSION

In poultry, the function of the thyroid is generally similar to typical vertebrates. The thyroid is involved in the regulation of reproduction, gonadal development, and egg production (McNabb, 2007). In present experiment, the difference in egg production between GP and DP was extremely significant ( $P < 0.01$ ), with an average of 100 eggs in GP (94–112) and 30 eggs in DP (2–50). RNA-seq revealed gene expression mechanisms and key signaling pathways in the thyroid and ovarian stroma of GP and DP, and a total of 1,114 and 733 DEGs were identified, respectively.

To further reveal the key molecules and the underlying regulatory mechanisms, we performed the GO enrichment analyses, which showed the BP category was allocated more DEGs than CC and MF. The BP

may be more important for egg-laying performance. This is consistent with previously reported results (Mishra et al., 2020). The genes enriched in the BP category of this study, including *GABRA1*, *LPAR2*, and *ATF3*, which have been reported to be possibly involved in regulating egg-laying performance (Bello et al., 2021; Chen et al., 2021), and *GABRA1* can inhibit the proliferation of granulosa cells and stimulate apoptosis (Sun et al., 2021).

Furthermore, through analyzing the GO results, 3 common terms were found in the top 5 terms with the highest significant level of two tissues, including extracellular space, calcium ion binding, and integral component of plasma membrane. A previous study on bulls has shown that high concentrations of extracellular space transcripts characterized high-fertility bull-derived spermatozoa and it could be associated with bull fertility (Feugang et al., 2010). The calcium ion binding has been identified in comparative transcriptome analyses of the estrus ovaries from yak and cattle as the most enriched terms in the MF category (Lan et al., 2016). The calcium ions, as second intracellular messengers, regulate many important physiological and pathological processes in cells. In addition to the participation of hormones and growth factors, calcium ions are also closely

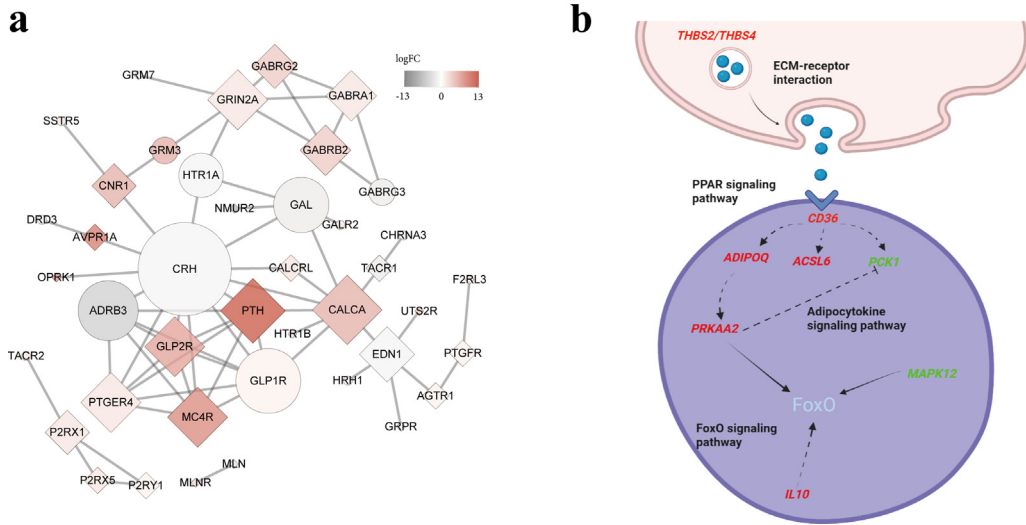


**Figure 3.** The PPI and schematic diagram of the molecular mechanism. (a) The PPI of DEGs on neuroactive ligand-receptor interaction. Squares represent genes differentially expressed in the thyroid, circles represent genes differentially expressed in the ovarian stroma, and the color scale bars indicated the fold change. (b) Schematic diagram of the possible regulation of ovarian development by ECM-receptor interaction, red represents up-regulated genes and green represents down-regulated genes. Abbreviations: PPI, protein-protein interaction; DEG, differentially expressed gene.

involved in the regulation of meiotic maturation of oocytes in mammals (Rozinek et al., 2006). It suggests that the regulation of meiotic maturation in the oocytes by the thyroid may exist differently between GP and DP ovaries. The plasma membrane defines the boundary separating the intracellular and extracellular environments, and mediates the interactions between a motile cell and its environment, and the integral component of plasma membrane can actively participate in all aspects of the motility process (Keren, 2011). For example, the adhesion-related categories, hormone-related categories, and cation transmembrane transport-related categories.

The KEGG enrichment analysis revealed 8 common pathways that significantly enriched both in the thyroid and ovarian stroma, the neuroactive ligand-receptor interaction had the highest significant level in both tissues. This result is similar to a study that confirmed

that the neuroactive ligand-receptor interaction pathway is essential for egg production in geese (Ouyang et al., 2020). Previous transcriptomic studies in zebrafish (Chen et al., 2019), rat (Xu et al., 2021), pig (Xu et al., 2015), goat (Su et al., 2018), duck (Tao et al., 2017), and chicken (Zhang et al., 2019) have also demonstrated the important role of this pathway in controlling ovarian function, egg-laying performance and other reproductive activities. Thus, the neuroactive ligand-receptor interaction pathway may be considered as an underlying molecular pathway within the thyroid to regulate ovarian stroma and affecting egg-laying performance between GP and DP.

In our study, by analyzing the PPI network of DEGs enriched in this pathway of 2 tissues, *PTH* and *CRH* may be the potential candidate genes affecting ovarian function and egg-laying performance because they were

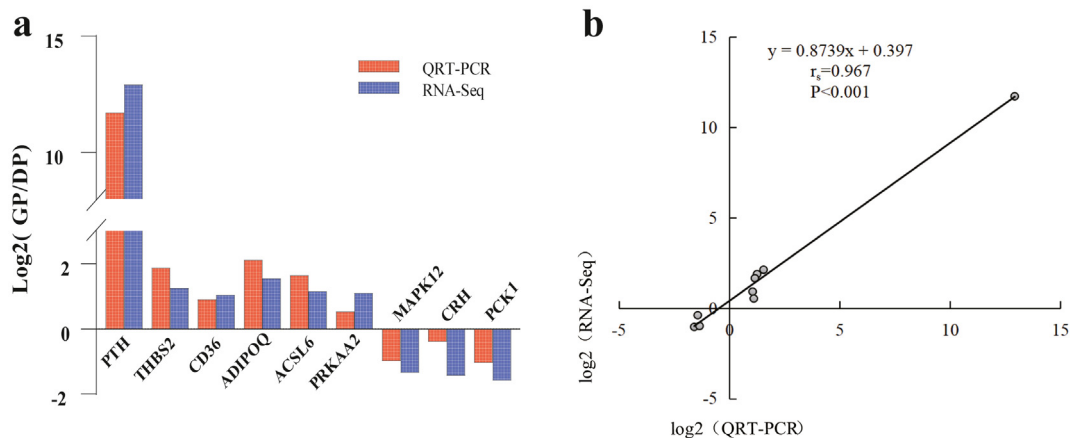


**Figure 4.** Validation of selected DEGs by qRT-PCR. (a) Comparison of mRNA expression levels. (b) Linear regression relationship between qRT-PCR and RNA-seq. Abbreviations: DEG, differentially expressed gene; qRT-PCR, quantitative real-time PCR; RNA-seq, transcriptome sequencing.

located in the core position of the regulatory networks. The *PTH* was up-regulated in the thyroid with a fold change up to 12.9.

The *PTH* encodes parathyroid hormone proprotein, which is processed for binding to PTH or PTH-related peptide receptors and is involved in regulating blood calcium and phosphorus levels (Khundmiri et al., 2016). Meanwhile, it has also been shown that PTH or PTH-related peptides can increase steroid secretion in rats (Rafferty et al., 1983), humans (Mazzocchi et al., 2001), and chickens (Rosenberg et al., 1987; Kawashima et al., 2005). Both calcium and phosphorus cycling and steroid metabolism are important for normal reproductive activity in poultry, which suggests that *PTH* may be important in thyroid regulation of ovarian function and egg-laying performance but rarely mentioned in other studies.

*CRH* has the highest number of nodes and directly linked to *PTH* with opposite expression trends. The *CRH* encodes adrenocorticotropin-releasing hormone which may be a downstream gene regulated by *PTH*. In addition, CRH is usually produced as an autocrine or paracrine inflammatory cytokine at peripheral inflammatory sites (Karalis et al., 1991) and may play a pro-inflammatory role by activating mast cells (Kempuraj et al., 2004). On the other hand, ovarian CRH was found not only in the theca and stroma, but also in the cytoplasm of human oocytes (Mastorakos et al., 1994). It may be involved in ovarian aseptic inflammatory processes (Nezi et al., 2000) caused by ovulation, and *PTH* may also be engaged in regulating this process.

The thrombospondin (THBS) family belongs to ECM proteins, which is consisted of 5 multidomain glycoproteins. And the *THBS2* and *THBS4* are grouped in the same class as they show high structural homology. In present study, genes involved in the ECM-receptor interaction of the thyroid that encode extracellular matrix components were up-regulated (*LAMA3*, *CHAD*, *THBS2*, *THBS4*), may directly affects BP within the ovary, such as folliculogenesis, ovulation, and steroidogenesis (Kulus et al., 2021). In a study on bovine corpus luteum, the ECM-receptor interaction was identified to be important in controlling ovarian cell development and function (Kliem et al., 2007), which is consistent with our findings in the pathway.

*CD36* is a specific receptor of thrombospondin 2/4 encoded by *THBS2* and *THBS4*, and their binding may cause changes in the expression of the PPAR signaling pathway, Adipocytokine signaling pathway, and FoxO signaling pathway in the ovarian stroma. A recent study has revealed that *THBS* and its receptor *CD36* expression gradually decreases with the maturation of follicles, and they may have an important impact on the ovarian function of bovine (Berisha et al., 2016).

*ADIPOQ*, *ACSL6*, and *PCK1*, as downstream genes of *CD36*, were differentially expressed in the PPAR signaling pathway of the ovarian stroma. The expression level of *ADIPOQ* was correlated with the level of adiponectin, an important adipocyte factor involved in the regulation of reproduction (Michalakis and Segars, 2010). In geese,

it has been proved that adiponectin can increase the secretion of P4 and weakly inhibit the production of E2 by regulating the expression of steroidogenic genes in granulosa cells (Meng et al., 2019), and there are similar results in laying hens (Li et al., 2021). The *ACSL6* encodes acyl-CoA synthetase long-chain family member 6, which is involved in lipid metabolism, and acyl-CoA synthase 6 regulates the long-chain polyunsaturated fatty acid composition of sperm cell membrane phospholipids and supports normal spermatogenesis in mice (Shishikura et al., 2019), while it has been shown that acyl-coenzyme A synthase 6 is associated with early ovarian aging (Kang et al., 2009).

*PCK1*, which can encode phosphoenolpyruvate carboxykinase 1, has been identified in ducks as a key gene in regulating gluconeogenesis and glycerol isogenesis, participated in maintaining glucose homeostasis and lipid storage (Chen et al., 2017). Hakimi et al. found that the *PCK1* knockout mice developed severe hypoglycemia and even died after birth (Hakimi et al., 2005). The effect of *PCK1* on reproduction needs to be further investigated.

*PRKAA2* encodes the protein kinase AMP-activated catalytic subunit alpha 2, and conditional ablation of *PRKAA1/2* leads to early reproductive aging in mice (Griffiths et al., 2020). Normal expression of *PRKAA1/2* is required to maintain female fertility, and the number of litters was significantly reduced in *PRKAA1/2* double-conditioned knockout mice (McCallum et al., 2018). The *PRKAA2* was mainly expressed in the ovarian stroma of high egg production ducks and may have an important regulatory role in the egg production mechanism of ducks.

In summary, our results suggest that the thyroid may act on the ovary through the neuroactive ligand-receptor interaction and ECM-receptor interaction to regulate egg-laying performance in ducks, nine key DEGs (*PTH*, *THBS2*, *THBS4*, *CD36*, *ADIPOQ*, *ACSL6*, *PRKAA2*, *CRH*, and *PCK1*) are important in this process, these pathways and DEGs may provide some new insights into the mechanism of thyroid regulation of ovarian function and egg production.

## ACKNOWLEDGMENTS

This research was supported by the Key Technology Support Program of Sichuan Province (2021YFYZ0014), and the China Agricultural Research System (CARS-42-4) for the financial support.

## DISCLOSURES

None.

## REFERENCES

- Bao, X., Y. Song, T. Li, S. Zhang, L. Huang, S. Zhang, J. Cao, X. Liu, and J. Zhang. 2020. Comparative transcriptome profiling of ovary tissue between black muscovy duck and white muscovy duck with high-and low-egg production. *Genes* 12:57.



- Bello, S. F., H. Xu, L. Guo, K. Li, M. Zheng, Y. Xu, S. Zhang, E. J. Bekele, A. A. Bahareldin, and W. Zhu. 2021. Hypothalamic and ovarian transcriptome profiling reveals potential candidate genes in low and high egg production of white Muscovy ducks (*Cairina moschata*). *Poult. Sci.* 100:101310.
- Berisha, B., D. Schams, D. Rodler, F. Sinowatz, and M. W. Pfaffl. 2016. Expression and localization of members of the thrombospondin family during final follicle maturation and corpus luteum formation and function in the bovine ovary. *J. Reprod. Dev.* 62:501–510.
- Bilezikian, J. P., J. N. Loeb, and D. E. Gammon. 1980. Induction of sustained hyperthyroidism and hypothyroidism in the turkey: physiological and biochemical observations. *Poult. Sci.* 59:628–634.
- Brady, K., H.-C. Liu, J. A. Hicks, J. A. Long, and T. E. Porter. 2020. Transcriptome analysis of the hypothalamus and pituitary of turkey hens with low and high egg production. *BMC Genomics* 21:1–17.
- Brady, K., H.-C. Liu, J. A. Hicks, J. A. Long, and T. E. Porter. 2021. Transcriptome analysis during follicle development in Turkey hens with low and high egg production. *Front. Genet.* 12:619196.
- Chen, H., W. Feng, K. Chen, X. Qiu, H. Xu, G. Mao, T. Zhao, Y. Ding, and X. Wu. 2019. Transcriptomic analysis reveals potential mechanisms of toxicity in a combined exposure to dibutyl phthalate and diisobutyl phthalate in zebrafish (*Danio rerio*) ovary. *Aquat. Toxicol.* 216:105290.
- Chen, X., X. Sun, I. M. Chimbaka, N. Qin, X. Xu, S. Liswaniso, R. Xu, and J. M. Gonzalez. 2021. Transcriptome analysis of ovarian follicles reveals potential pivotal genes associated with increased and decreased rates of chicken egg production. *Front. Genet.* 12:622751.
- Chen, L., T. Zeng, G. Q. Li, R. Liu, Y. Tian, Q. H. Li, and L. Z. Lu. 2017. PCK1 expression is correlated with the plasma glucose level in the duck. *Anim. Genet.* 48:358–361.
- Feugang, J., N. Rodriguez-Osorio, A. Kaya, H. Wang, G. Page, G. Ostermeier, E. Topper, and E. Memili. 2010. Transcriptome analysis of bull spermatozoa: implications for male fertility. *Reprod. Biomed. Online* 21:312–324.
- Griffiths, R. M., C. A. Pru, S. K. Behura, A. R. Cronrath, M. L. McCallum, N. C. Kelp, W. Winuthayanon, T. E. Spencer, and J. K. Pru. 2020. AMPK is required for uterine receptivity and normal responses to steroid hormones. *Reproduction* 159:707–717.
- Haddad, E. E., and M. M. Mashaly. 1989. Effect of thyroidectomy of immature male chickens on circulating thyroid hormones and on response to thyroid-stimulating hormone and chronic cold exposure. *Poult. Sci.* 68:169–176.
- Hakimi, P., M. T. Johnson, J. Yang, D. F. Lepage, R. A. Conlon, S. C. Kalhan, L. Reshef, S. M. Tilghman, and R. W. Hanson. 2005. Phosphoenolpyruvate carboxykinase and the critical role of cataplerosis in the control of hepatic metabolism. *Nutr. Metab. (Lond)* 2:33.
- Hu, Z., J. Liu, J. Cao, H. Zhang, and X. Liu. 2021. Ovarian transcriptomic analysis of black Muscovy duck at the early, peak and late egg-laying stages. *Gene* 777:145449.
- Huang, X., W. Zhou, H. Cao, H. Zhang, X. Xiang, and Z. Yin. 2022. Ovarian transcriptomic analysis of Ninghai indigenous chickens at different egg-laying periods. *Genes* 13:595.
- Kang, H., S. K. Lee, M. H. Kim, H. Choi, S. H. Lee, and K. Kwack. 2009. Acyl-CoA synthetase long-chain family member 6 is associated with premature ovarian failure. *Fertil. Steril.* 91:1339–1343.
- Karalis, K., H. Sano, J. Redwine, S. Listwak, R. L. Wilder, and G. P. Chrousos. 1991. Autocrine or paracrine inflammatory actions of corticotropin-releasing hormone in vivo. *Science* 254:421–423.
- Kawashima, M., T. Takahashi, H. Yanai, H. Ogawa, and T. Yasuoka. 2005. Direct action of parathyroid hormone-related peptide to enhance corticosterone production stimulated by adrenocorticotropin hormone in adrenocortical cells of hens. *Poult. Sci.* 84:1463–1469.
- Kempuraj, D., N. G. Papadopoulou, M. Lytinas, M. Huang, K. Kandere-Grzybowska, B. Madhappan, W. Boucher, S. Christodoulou, A. Athanassiou, and T. C. Theoharides. 2004. Corticotropin-releasing hormone and its structurally related urocortin are synthesized and secreted by human mast cells. *Endocrinology* 145:43–48.
- Keren, K. 2011. Cell motility: the integrating role of the plasma membrane. *Eur. Biophys. J.* 40:1013–1027.
- Khundmiri, S. J., R. D. Murray, and E. Lederer. 2016. PTH and vitamin D. *Compr. Physiol.* 6:561–601.
- Kim, D., B. Langmead, and S. L. Salzberg. 2015. HISAT: a fast spliced aligner with low memory requirements. *Nat. Methods* 12:357–360.
- Kliem, H., H. Welter, W. D. Kraetzl, M. Steffl, H. H. Meyer, D. Schams, and B. Berisha. 2007. Expression and localisation of extracellular matrix degrading proteases and their inhibitors during the oestrous cycle and after induced luteolysis in the bovine corpus luteum. *Reproduction* 134:535–547.
- Kulus, J., M. Kulus, W. Kranc, K. Jopek, M. Zdun, M. Józkwiaik, J. M. Jaśkowski, H. Piotrowska-Kempisty, D. Bukowska, and P. Antosik. 2021. Transcriptomic profile of new gene markers encoding proteins responsible for structure of porcine ovarian granulosa cells. *Biology* 10:1214.
- Lan, D., X. Xiong, C. Huang, T. D. Mipam, and J. Li. 2016. Toward understanding the genetic basis of yak ovary reproduction: a characterization and comparative analyses of estrus ovary transcriptome in yak and cattle. *PLoS One* 11:e0152675.
- Li, H., B. Handsaker, A. Wysoker, T. Fennell, J. Ruan, N. Homer, G. Marth, G. Abecasis, and R. Durbin. 2009. The sequence alignment/map format and SAMtools. *Bioinformatics* 25:2078–2079.
- Li, J., X. J. Ma, X. Wu, S. J. Si, C. Li, P. K. Yang, G. X. Li, X. J. Liu, Y. D. Tian, and X. T. Kang. 2021. Adiponectin modulates steroid hormone secretion, granulosa cell proliferation and apoptosis via binding its receptors during hens' high laying period. *Poult. Sci.* 100:101197.
- Liao, Y., G. K. Smyth, and W. Shi. 2014. featureCounts: an efficient general purpose program for assigning sequence reads to genomic features. *Bioinformatics* 30:923–930.
- Lien, R., and T. Siopes. 1989. Effects of thyroidectomy on egg production, molt, and plasma thyroid hormone concentrations of turkey hens. *Poult. Sci.* 68:1126–1132.
- Ma, Z., K. Jiang, D. Wang, Z. Wang, Z. Gu, G. Li, R. Jiang, Y. Tian, X. Kang, and H. Li. 2021. Comparative analysis of hypothalamus transcriptome between laying hens with different egg-laying rates. *Poult. Sci.* 100:101110.
- Mastorakos, G., C. D. Scopa, A. Vryonidou, T. C. Friedman, D. Kattis, C. Phenekos, M. J. Merino, and G. P. Chrousos. 1994. Presence of immunoreactive corticotropin-releasing hormone in normal and polycystic human ovaries. *J. Clin. Endocrinol. Metab.* 79:1191–1197.
- Mazzocchi, G., F. Aragona, L. K. Malendowicz, and G. G. Nussdorfer. 2001. PTH and PTH-related peptide enhance steroid secretion from human adrenocortical cells. *Am. J. Physiol. Endocrinol. Metab.* 280:E209–E213.
- McCallum, M. L., C. A. Pru, A. R. Smith, N. C. Kelp, M. Foretz, B. Viollet, M. Du, and J. K. Pru. 2018. A functional role for AMPK in female fertility and endometrial regeneration. *Reproduction* 156:501–513.
- McNabb, F. A. 2007. The hypothalamic-pituitary-thyroid (HPT) axis in birds and its role in bird development and reproduction. *Crit. Rev. Toxicol.* 37:163–193.
- Meng, B., Z. Cao, Y. Gai, M. Liu, M. Gao, M. Chen, Z. Ning, and X. Luan. 2019. Effects of recombinant goose adiponectin on steroid hormone secretion in Huoyan geese ovarian granulosa cells. *Anim. Reprod. Sci.* 205:34–43.
- Michalakakis, K. G., and J. H. Segars. 2010. The role of adiponectin in reproduction: from polycystic ovary syndrome to assisted reproduction. *Fertil. Steril.* 94:1949–1957.
- Miller, B. F., P. E. Sanford, and R. E. Clegg. 1962. The effect of thyroxine on egg production and egg quality of normal and radio-thyroid-ectricized hens. *Poult. Sci.* 41:989–994.
- Mishra, S. K., B. Chen, Q. Zhu, Z. Xu, C. Ning, H. Yin, Y. Wang, X. Zhao, X. Fan, and M. Yang. 2020. Transcriptome analysis reveals differentially expressed genes associated with high rates of egg production in chicken hypothalamic-pituitary-ovarian axis. *Scient. Rep.* 10:1–8.
- Nezi, M., G. Mastorakos, Z. Mouslech, et al. 2000. Corticotropin releasing hormone and the immune/inflammatory response. *Endotext*. K. R. Feingold, ed. MDText.com, Inc., South Dartmouth (MA) MDText.com, Inc. Copyright © 2000-2022.
- Onagbesan, O., V. Bruggeman, and E. Decuypere. 2009. Intra-ovarian growth factors regulating ovarian function in avian species: a review. *Anim. Reprod. Sci.* 111:121–140.
- Ouyang, Q., S. Hu, G. Wang, J. Hu, J. Zhang, L. Li, B. Hu, H. He, H. Liu, and L. Xia. 2020. Comparative transcriptome analysis suggests key roles for 5-hydroxytryptamine receptors in control of goose egg production. *Genes* 11:455.

- Rafferty, B., J. M. Zanelli, M. Rosenblatt, and D. Schulster. 1983. Corticosteroidogenesis and adenosine 3', 5'- monophosphate production by the amino-terminal (1-34) fragment of human parathyroid hormone in rat adrenocortical cells. *Endocrinology* 113:1036–1042.
- Rosenberg, J., M. Pines, and S. Hurwitz. 1987. Response of adrenal cells to parathyroid hormone stimulation. *J. Endocrinol.* 112:431–437.
- Rozinek, J., R. Rajmon, J. Petr, J. Rohlik, M. Jeřeta, M. Sedmikova, D. Reháč, and F. Jilek. 2006. Ultrastructural localisation of calcium deposits in pig ovarian follicles. *Anim. Reprod. Sci.* 91:123–132.
- Sechman, A. 2013. The role of thyroid hormones in regulation of chicken ovarian steroidogenesis. *Gen. Comp. Endocrinol.* 190:68–75.
- Shishikura, K., S. Kuroha, S. Matsueda, H. Iseki, T. Matsui, A. Inoue, and M. Arita. 2019. Acyl-CoA synthetase 6 regulates long-chain polyunsaturated fatty acid composition of membrane phospholipids in spermatids and supports normal spermatogenic processes in mice. *Faseb J.* 33:14194–14203.
- Su, F., X. Guo, Y. Wang, Y. Wang, G. Cao, and Y. Jiang. 2018. Genome-wide analysis on the landscape of transcriptomes and their relationship with DNA methylomes in the hypothalamus reveals genes related to sexual precocity in jining gray goats. *Front. Endocrinol.* 9:501.
- Sun, X., X. Chen, J. Zhao, C. Ma, C. Yan, S. Liswaniso, R. Xu, and N. Qin. 2021. Transcriptome comparative analysis of ovarian follicles reveals the key genes and signaling pathways implicated in hen egg production. *BMC Genomics* 22:1–20.
- Tao, Z., W. Song, C. Zhu, W. Xu, H. Liu, S. Zhang, and L. Huifang. 2017. Comparative transcriptomic analysis of high and low egg-producing duck ovaries. *Poult. Sci.* 96:4378–4388.
- Xu, S., D. Wang, D. Zhou, Y. Lin, L. Che, Z. Fang, and D. Wu. 2015. Reproductive hormone and transcriptomic responses of pituitary tissue in anestrus gilts induced by nutrient restriction. *PLoS One* 10:e0143219.
- Xu, W., H. Wu, and L. Shang. 2021. Gene expression in rat placenta after exposure to di (2-ethylhexyl) phthalate. *Hum. Exp. Toxicol.* 40:504–514.
- Yan, X., H. Liu, J. Hu, X. Han, J. Qi, Q. Ouyang, B. Hu, H. He, L. Li, and J. Wang. 2022. Transcriptomic analyses of the HPG axis-related tissues reveals potential candidate genes and regulatory pathways associated with egg production in ducks. *BMC Genomics* 23:1–14.
- Zhang, T., L. Chen, K. Han, X. Zhang, G. Zhang, G. Dai, J. Wang, and K. Xie. 2019. Transcriptome analysis of ovary in relatively greater and lesser egg producing Jinghai Yellow Chicken. *Anim. Reprod. Sci.* 208:106114.
- Zhu, Z., Z. Miao, H. Chen, Q. Xin, L. Li, R. Lin, Q. Huang, and N. Zheng. 2017. Ovarian transcriptomic analysis of Shan Ma ducks at peak and late stages of egg production. *Asian-Austral. J. Anim. Sci.* 30:1215.